Interactions of rutin with oxidovanadium(IV) cation. Anticancer improvement effects of glycosylated flavonoids.

Helen Goitia, Patricia Quispe, Luciana G. Naso, Valeria R. Martínez, Marilin Rey, Alberto C. Rizzi, Evelina G. Ferrer, Patricia A.M. Williams*

New Journal of Chemistry

Supplementary material

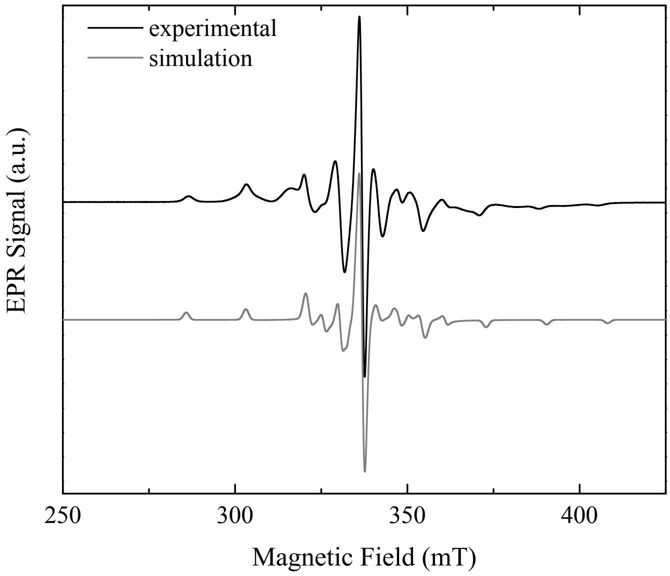

Figure S1. Experimental powder EPR spectrum of the $Na_2[VO(rut)(OH)_2].5H_2O$ complex obtained at 120 K (black) together with simulation (gray). Microwave frequency 9.4516 GHz. EPR parameters obtained by simulation: g_1 = 1.9869, g_2 = 1.9763, g_3 = 1.9477; A_1 = 28.7 x 10^{-4} cm^{-1}, A_2 = 51.7 x 10^{-4} cm^{-1}; A_3 = 158.9 x 10^{-4} cm^{-1}.

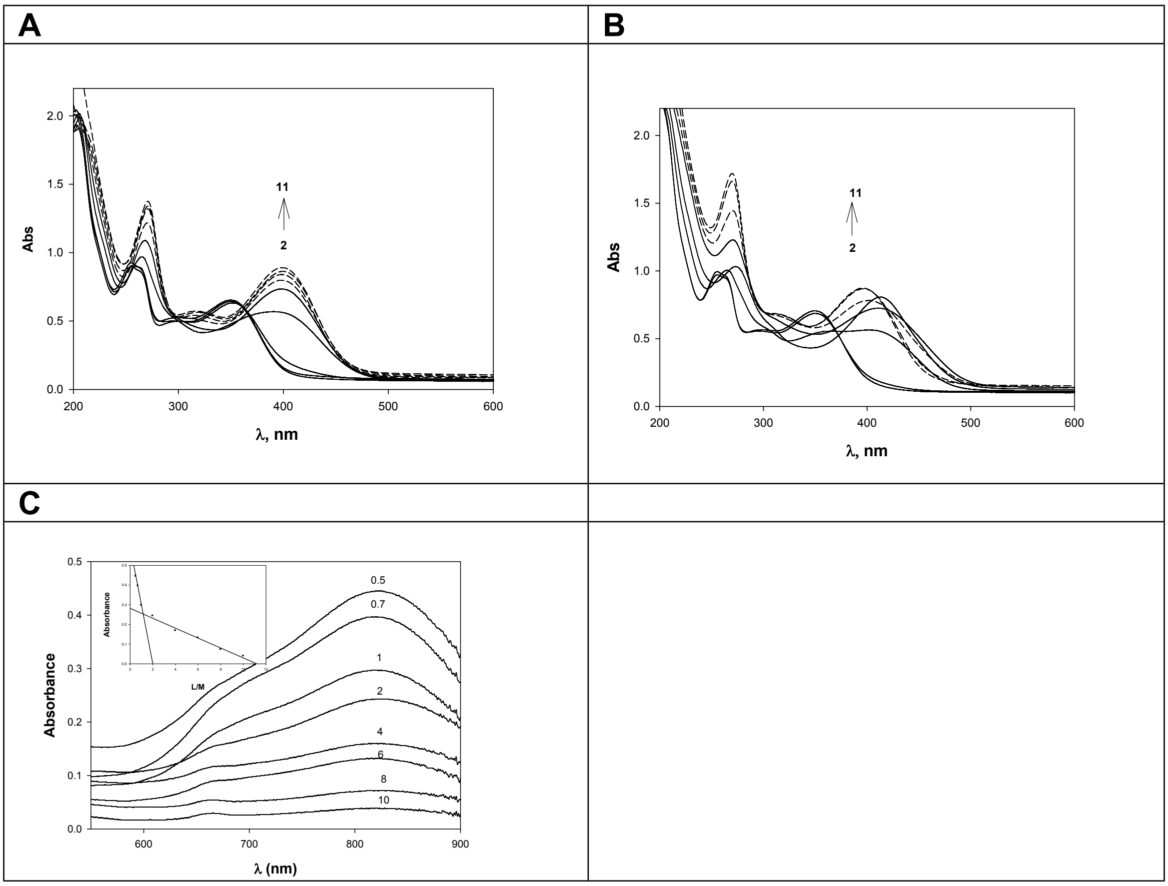

Figure S2. A) Spectra of rutin (4×10^{-5} M), aqueous solutions, at different pH values. B) Spectra of aqueous solutions of 5×10^{-5} M rutin and 2.5×10^{-5} M $VOCl_2$ at different pH values. C) UV-vis spectra of rutin (8×10^{-3} M) DMSO with the addition of aqueous solutions of $VOCl_2$ in ligand-to-metal ratios (L/M) from 10.0 to 0.7 (pH 7); nitrogen atmosphere. Inset: Spectrophotometric determination of VOrut complex stoichiometry at 820 nm.

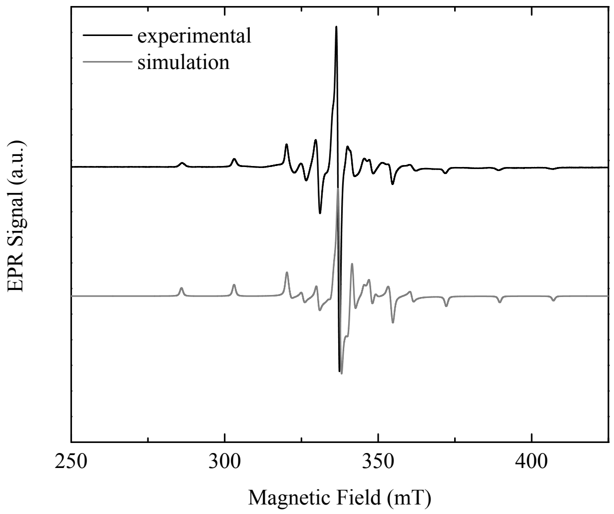

Figure S3. Frozen EPR spectra on DMSO solution of $[VO(rut)(OH)_2]Na_2.5H_2O$ complex (black) together with simulation (gray). Microwave frequency 9.46546 GHz. EPR parameters obtained by simulation: g_1 = 1.9873, g_2 = 1.9780, g_3 = 1.9510; A_1 = 26.0 x 10^{-4} cm^{-1}, A_2 = 52.0 x 10^{-4} cm^{-1}; A_3 = 157.7 x 10^{-4} cm^{-1}.

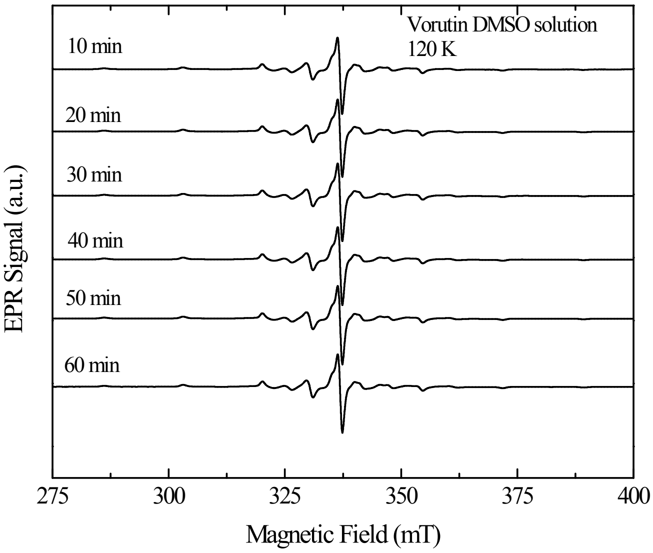

Figure S4. Frozen EPR spectra on DMSO solution of $[VO(rut)(OH)_2]Na_2.5H_2O$ recorded at 120K as a function of time.

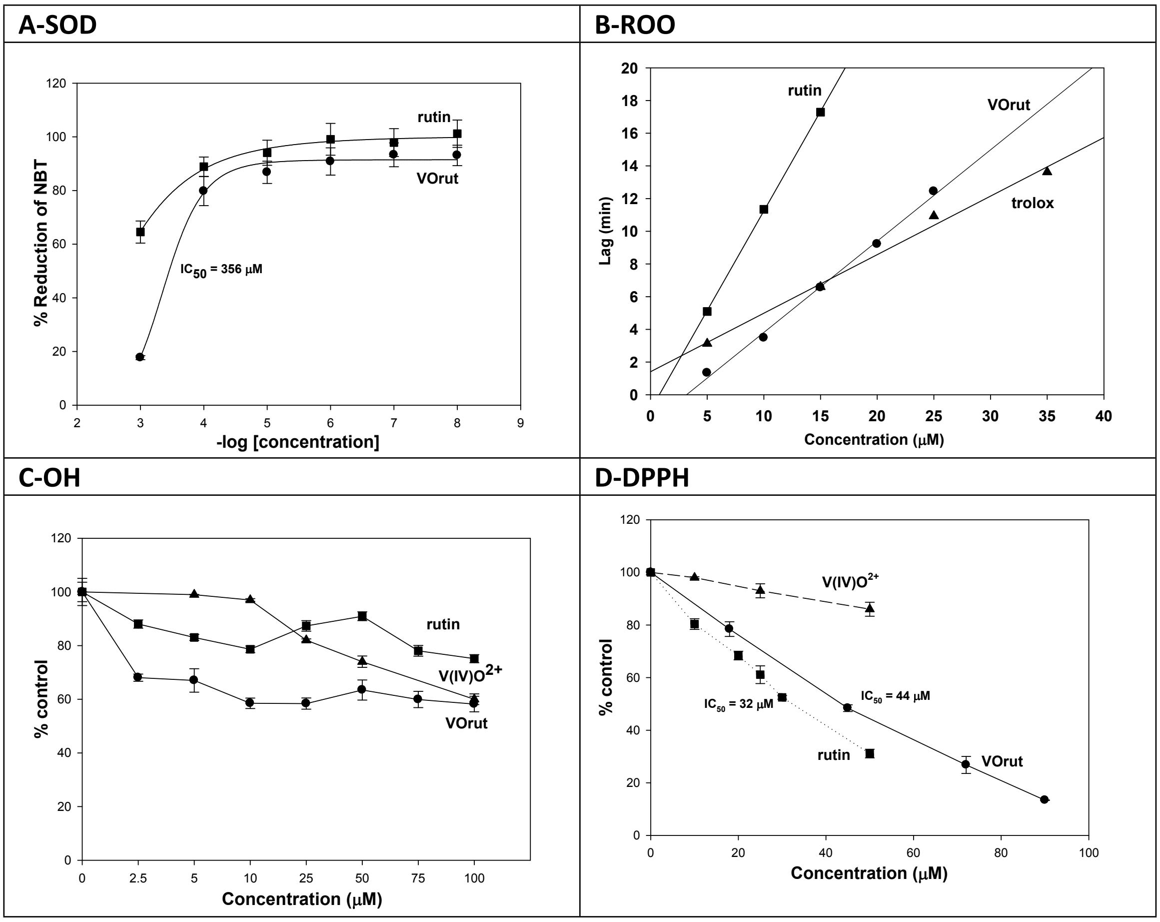

Figure S5. Effects of rutin, oxidovanadium(IV) cation and VOrut on: A) the reduction of nitroblue tetrazolium by the generated superoxide radical (phenazine methosulfate and reduced nicotinamide adenine dinucleotide system). B) peroxyl radicals generated by the thermal decomposition of AAPH (2,2-azobis(2-amidinopropane) dihydrochloride); lag phase is the delay of the consumption of the spectrometric probe, pyranine, calculated as the time due to the consumption of peroxyl radicals by the added compounds, before the consumption of pyranine started. C) extent of deoxyribose degradation by hydroxyl radical, measured with the thiobarbituric acid method. D) reduction of the concentration of 1,1-diphenyl-2-picrylhydrazyl radical. The values are expressed as the mean ± the standard error of at least three independent experiments.

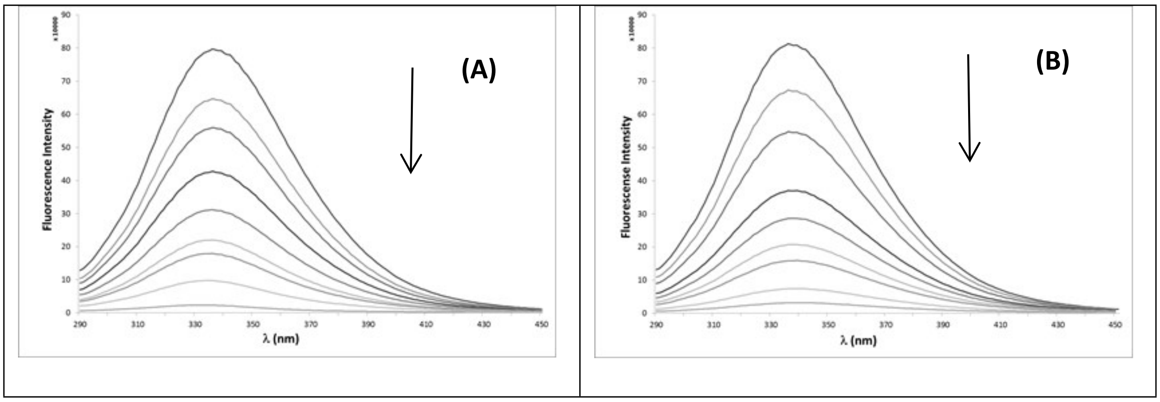

Figure S6. Fluorescence emission spectra of BSA (6 μM) with successive addition of rutin (A) and VOrut (B) at different concentrations (0, 5, 10, 20, 30, 40, 50, 75, 100 μM).

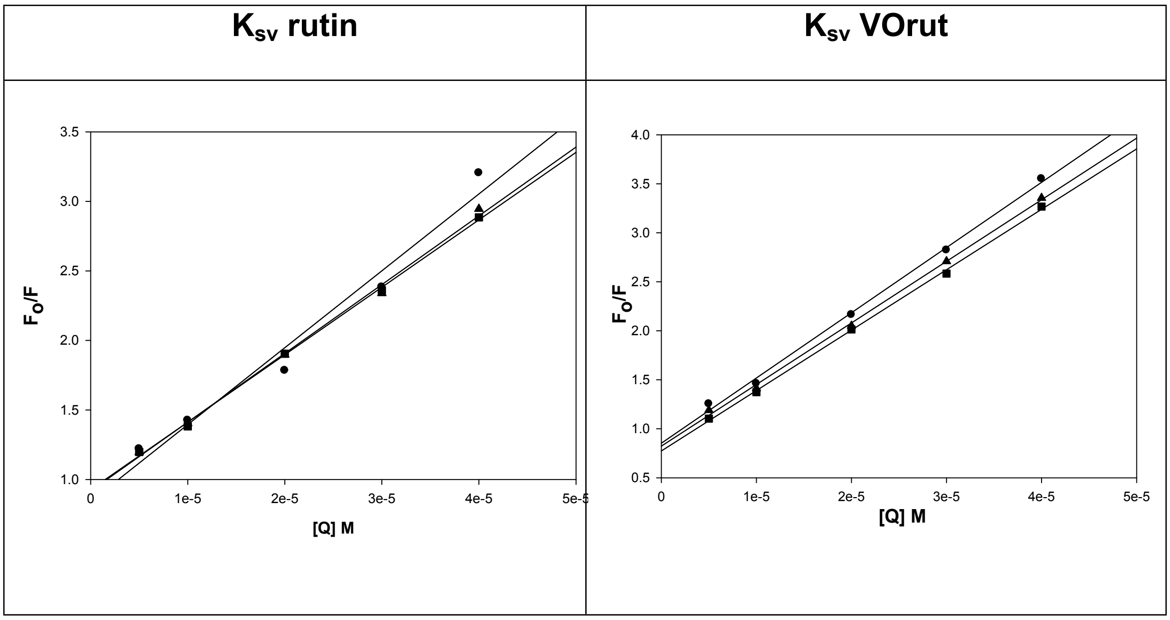

Figure S7. Plots of F_0/F vs [Q] for BSA with rutin and VOrut at different temperatures ((●), 298 K; (▲), 303 K; (■), 310 K), $\lambda_{ex} = 280$ nm.

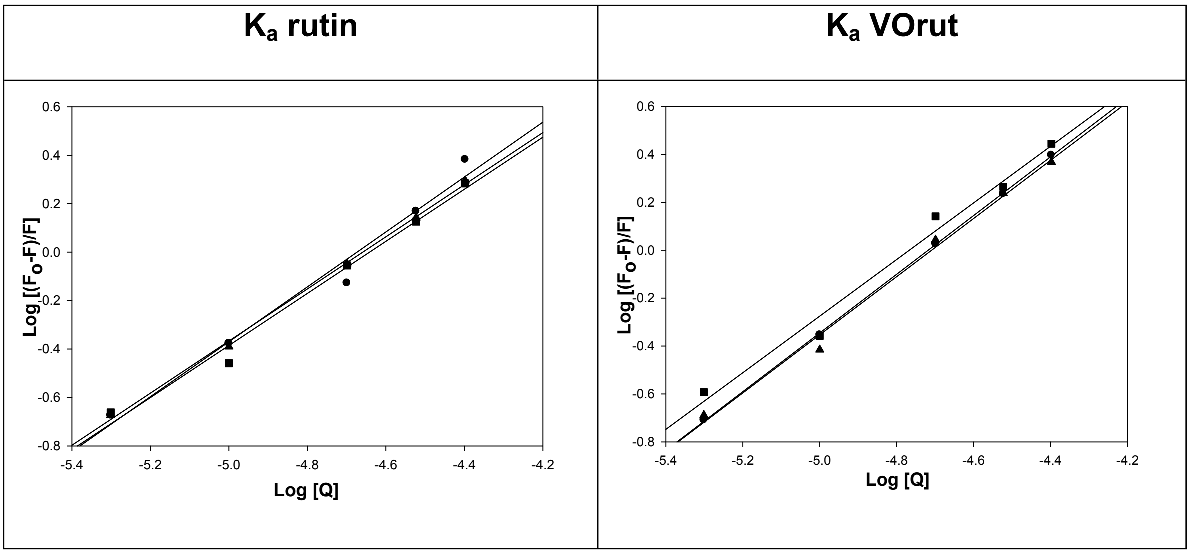

Figure S8. Plots of log(F_0 − F)/F vs. log [Q] for BSA with rutin and VOrut at different temperatures ((●), 298 K; (▲), 303 K; (■), 310 K), λ_{ex} = 280 nm

Table S1 Assignment of the main bands of the infrared spectra of rutin and the oxidovanadium(IV) complex, VOrut (band positions in cm^{-1})

Assignments	**[VO(OH)$_2$(Rut)]Na$_2$**	**Rutin**
ν(O–H)	3414, br	3422, br
ν(C=O)	1650, vs	1656, s
ν(C=C)	1577, s	1601, s
ν(C=C), ring B	1485, s	1505, s
δ_{ip}(O-H)	1361, s	1361, s
δ(C-O-H)	1272, s	1296, s
ν(C–O–C)	1205, m	1205, m
ν(C-O)$_{endo}$	1013, w	1013, s
ν(V=O)	920, w	

Br, broad; s, strong; m, medium; w, weak; sh, shoulder.